Performances of Marcum's (S + N)–N Integration Scheme with Fluctuating Targets

ALEXANDER SADOGURSKY, Member, IEEE
NADAV LEVANON, Life Fellow, IEEE
Tel Aviv University

The performances of Marcum's (signal + noise) − noise ((S + N)−N) integration scheme are analyzed for SW1 and SW2 fluctuating targets. This lesser known integration concept was not treated by Swerling when he extended Marcum's main signal + noise integration to four cases of fluctuating targets. We present closed-form probability density (pdfs) functions confirmed and extended by simulations. We show typical signal-to-noise ratio (SNR) loss of 1 dB for both SW1 and SW2, agreeing with Marcum's result for SW0. (S + N)−N integration is inherent in our work on noncoherent pulse compression, hence the renewed interest.

Manuscript received September 28, 2012; revised February 5, 2013; released for publication June 8, 2013.

IEEE Log No. T-AES/50/1/944791.

DOI. No. 10.1109/TAES.2013.120614.

Refereeing of this contribution was handled by S. Watts.

Author's address: A. Sadogursky, Marvell Semiconductor Israel Ltd.; N. Levanon, Department of Electrical Engineering–Systems, Tel Aviv University, PO Box 39040, Tel Aviv, 69978, Israel, E-mail: (nadav@eng.tau.ac.il).

I. INTRODUCTION

In his seminal 1947 research memorandum [1], J. I. Marcum laid the basics of noncoherent integration of radar returns from nonfluctuating targets. A section of that memorandum is devoted to a special noncoherent integration scheme

> *. . . in which a pulse known to be only noise is subtracted from each possible signal plus noise pulse. M of these composite pulses are then integrated. With no signal, the average value of any number of such composite pulses is nearly zero . . ..*

Effectively (signal + noise) − noise (S + N)−N integration scheme uses a mismatched reference, and some detection loss is expected. In the Appendix to his research memorandum (following (184)), Marcum states that

> *There appears to be no significant difference in the probabilities of detection for M between 1 and 10 (pulses). For M between 100 and 1000, the composite case gives an effective signal-to-noise ratio about 1 dB lower than the ordinary case.*

P. Swerling [2] extended Marcum's work to fluctuating targets, but did not include in his extension the (S + N)−N integration scheme.

In this paper we analyzed (S + N)−N detection performances for Swerling 1 and Swerling 2 fluctuating targets. Theoretical expressions were developed for the probability density functions (pdf) as a function of signal-to-noise ratio (SNR) and the number of integrated composite pulses (M). The theoretical expressions were confirmed by Monte-Carlo simulations. Probability of detection (P_{D}) as a function of SNR were obtained by simulations, with the probability of false alarm (P_{FA}) and M as parameters.

II. MOTIVATION

Marcum's (S + N)−N integration is inherent in our work on noncoherent pulse compression [3-6]. The concept is demonstrated in Fig. 1, which shows noncoherent pulse compression based on Barker 13. The top subplot displays the transmitted signal, constructed from 13 subpulses. It is an ON-OFF keyed unipolar signal obtained by Manchester encoding a Barker 13 code. Such a unipolar signal can be generated by noncoherent source (e.g., magnetrons, lasers, optical masks, etc.). The top subplot also represents the envelope-detected reflection from a point target before noise is added. The middle subplot displays the reference signal, stored in the receiver, with which the received signal is correlated. The normalized cross-correlation is plotted in the lower subplot. The positive part of the cross-correlation, the only part used as an output, resembles the autocorrelation of a bipolar Barker 13 signal. The similar outputs mean that shape-wise noncoherent pulse compression yields results similar to coherent pulse compression.

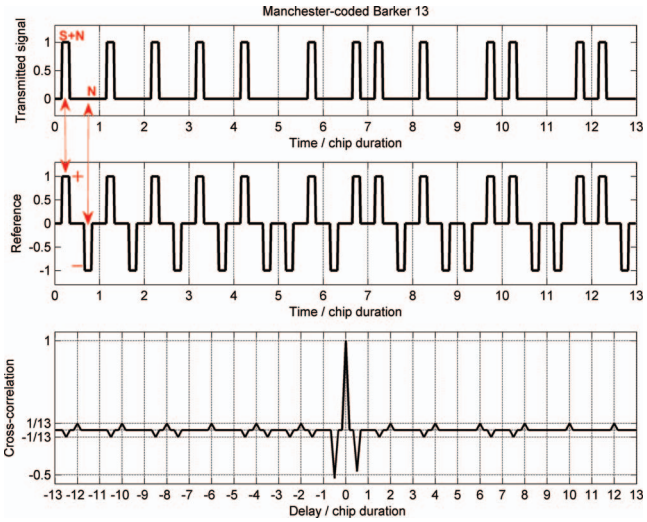

Fig. 1. Transmitted pulses (top), reference signal (middle), resulting cross-correlation (bottom). Based on Barker 13 [1 1 1 1 1 -1 -1 1 1 -1 1 -1 1].

The arrows and labels inserted in Fig. 1 explain the relation to (S + N)–N integration. At delay = 0 the signal and reference are aligned as plotted. Note that each returned pulse (the first one is marked as S + N) is multiplied by a positive reference pulse. All the negative reference pulses multiply noise-only receptions (the first one is marked as N). This is an implementation of Marcum's alternative integration scheme, analyzed in the present paper. Noncoherent pulse compression based on minimum peak sidelobe (MPSL) binary code of length 1112 was recently implemented in a laser range finder [6].

A periodic case was recently demonstrated using magnetron marine radar [5]. Periodic groups of 8 pulses were ON-OFF modulated according to Manchester-coded Barker 4. The transmitted periodic sequence was {0 1 1 0 1 0 1 0}, where "1" implies a transmitted pulse and "0" implies an omitted pulse. The corresponding reference sequence in the receiver was $\{-1\ 1\ 1\ -1\ 1\ -1\ 1\ -1\}$. In each period of 8 pulse repetition intervals (PRIs), 4 receptions when no pulse was transmitted are subtracted from 4 reflections of transmitted pulses. The periodic cross-correlation between the two sequences is ideal {1 0 0 0 0 0 0 0}, implying an extension of the unambiguous delay to 8 × PRI. In addition to ON-OFF coding based on Barker 4, [5] shows results based on Ipatov 5 binary code, which results in an extension of the unambiguous delay to 5 × PRI. Another important advantage of (S + N)–N integration, demonstrated in the field trials [5], is the zero-centered noise-only output. Conventional (S + N) noncoherent integration was implemented simultaneously by using a reference periodic sequence identical to the transmitted periodic sequence. The mean of its noise-only output is not zero but depends on the noise level and the number of pulses integrated. Fig. 2 presents detection of a small boat in calm sea at a range of 1.2 km, from coastal magnetron radar. Both (S + N) and (S + N)–N integration results are shown. The

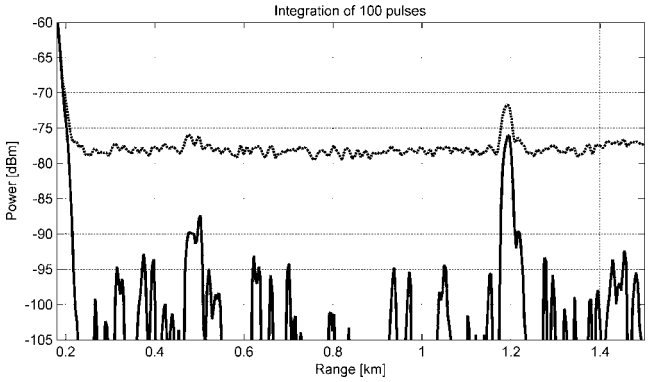

Fig. 2. Small boat detection by coastal magnetron marine radar using conventional (S + N) integration (dash) and (S + N)–N integration (solid).

need to quantify the SNR loss of the (S + N)–N integration, relative to the conventional (S + N) integration, prompted the analysis presented in the following sections.

Note in Fig. 2 that at short range (< 0.2 km), near-clutter returns are stronger than thermal noise. In that case off-target detection produces (C + N)–N ((clutter + noise)−noise), which is not centered around zero. C represents clutter return.

TERMINOLOGY

z Normalized output of a square-law detector.
M Number of pulses or composite pulses.
$y = \sum_{i=1}^{M} z_i$ Sum of M outputs.
ω Fourier variable.
σ^2 Noise variance.
A Amplitude of the received signal.
$SNR = x = \frac{A^2}{2\sigma^2}$ Input signal-to-noise ratio.
$\overline{x} = \frac{A_0^2}{\sigma^2}$ Average input SNR ratio for Rayleigh-distributed fluctuating target.
y_T Detection threshold for y.

III. MARCUM'S RESULTS FOR SQUARE-LAW DETECTION OF NONFLUCTUATING TARGETS (SWERLING 0)

When the output of a single detected pulse following square-law detector

$$r^2 = (A + n_I)^2 + n_Q^2, \quad n_{I,Q} : \mathrm{N}\left(0, \sigma^2\right) \tag{1}$$

is normalized according to

$$z = \frac{r^2}{2\sigma^2} \tag{2}$$

then the pdf of z is given by [1]

$$p\left(z|\, A\right) = \exp\left[-\left(z + \frac{A^2}{2\sigma^2}\right)\right] \mathrm{I}_0\left[\sqrt{\frac{2zA^2}{\sigma^2}}\right]. \tag{3}$$

I_0 is the modified Bessel function. Using the expression for *SNR*

$$x = \frac{A^2}{2\sigma^2} \tag{4}$$

(3) becomes

$$p\,(z|\,x) = e^{(-z-x)}\mathrm{I}_0\left[2\sqrt{xz}\right]. \tag{5}$$

The corresponding characteristic function is

$$C_1\,(\omega) = \frac{e^{-x}}{1+\omega}e^{\frac{x}{1+\omega}}. \tag{6}$$

The characteristic function of the sum of M independent detected pulses is

$$C_M\,(\omega) = [C_1\,(\omega)]^M = \frac{e^{-Mx}}{(1+\omega)^M}e^{\frac{Mx}{1+\omega}}. \tag{7}$$

The inverse transform yields the pdf of y (the sum of M normalized detected pulses z)

$$p\,(y|\,x) = \left(\frac{y}{Mx}\right)^{\frac{M-1}{2}} e^{(-y-Mx)} \times \mathrm{I}_{M-1}\left[2\sqrt{Mxy}\right],\ y \geq 0,\ \text{zero elswhere.} \tag{8}$$

Setting $x = 0$ in (7) yields the noise-only case

$$C_{M\,\text{noise}}\,(\omega) = \frac{1}{(1+\omega)^M}. \tag{9}$$

The corresponding noise-only pdf is

$$p\,(y) = \frac{y^{M-1}e^{-y}}{(M-1)!}, \quad y \geq 0, \quad \text{zero elsewhere.} \tag{10}$$

For the noise-only case we can derive a closed-form expression of the probability of crossing a threshold. Thus integrating (10) yields the probability of false alarm

$$P_{\mathrm{FA}} = \int_{y_T}^{\infty} \frac{y^{M-1}e^{-y}}{(M-1)!}dy \;=\; e^{-y_T}\sum_{k=0}^{M-1}\frac{y_T^k}{k!}. \tag{11}$$

The threshold y_T can be extracted from (11) using a simple MATLAB line suggested by Chernyak [7]:

$$\mathrm{y_T} = 0.5\ *\,\mathrm{chi2inv}\,(1-\mathrm{P_{FA}}\,,\ 2*\mathrm{M})\,. \tag{12}$$

IV. (S + N)–N INTEGRATION FOR NONFLUCTUATING TARGET (SWERLING 0)

The (S + N)–N noncoherent integration output can be expressed as

$$r^2 = \underbrace{\sum_{m=1,3,5..}^{2M-1}\left[(A+n_{Im})^2+n_{Qm}^2\right]}_{a} + \underbrace{\left(-\sum_{m=2,4,6..}^{2M}\left[n_{Im}^2+n_{Qm}^2\right]\right)}_{b}. \tag{13}$$

The first term on the right hand side (RHS) of (13) is the sum of M signal-plus-noise pulses. The second term is the sum of M negative noise pulses. Using the results in Section III, and applying $\alpha = -1$ to the Fourier transform rule

$$p(t) \Leftrightarrow C\,(\omega)\,, \quad p(\alpha t) \Leftrightarrow C\,(\omega/\alpha) \tag{14}$$

we get the characteristic function corresponding to the pdf of the sum in (13)

$$C_{SNN}\,(\omega) = \frac{e^{-Mx}}{(1+\omega)^M}e^{\frac{Mx}{1+\omega}}\ \frac{1}{(1-\omega)^M} = \frac{e^{-Mx}}{\left(1-\omega^2\right)^M}e^{\frac{Mx}{1+\omega}}. \tag{15}$$

Marcum's memorandum includes closed-form expressions for either noise only, or signal plus noise when $M = 1$. For the noise-only case setting $x = 0$ in (15) yields

$$C_{\text{noise}}(\omega) = \frac{1}{(1-\omega^2)^M} \tag{16}$$

resulting in the pdf of y for noise-only

$$p\,(y) = \frac{1}{\sqrt{\pi}\,(M-1)!}\left|\frac{y}{2}\right|^{M-\frac{1}{2}}\mathbf{K}_{M-\frac{1}{2}}\,|y| \tag{17}$$

where $\mathbf{K}$ is the modified Bessel function of the 2nd kind. For (S + N)–N, but $M = 1$, we get

$$p\,(y|\,x) = \begin{cases} \frac{e^{y-\frac{x}{2}}}{2}\mathbf{Q}\left(\sqrt{x}, 2\sqrt{y}\right), & y > 0 \\ \frac{e^{y-\frac{x}{2}}}{2}, & y \leq 0 \end{cases} \tag{18}$$

where $\mathbf{Q}$ is Marcum's $\mathbf{Q}$ equation.

Marcum did not reach a closed-form expression for the general case of nonfluctuating targets ($M > 1$, $x > 0$). We do not attempt to try this. Therefore, numerical results with nonfluctuating targets (SW0) are obtained using Monte Carlo simulations.

Fortunately we were able to get closed-form expressions for Rayleigh-distributed fluctuating targets (SW1 and SW2) for the general case ($M \geq 1$, $x \geq 0$). These results follow, starting with $M = 1$.

V. (S + N)–N SINGLE PULSE PROCESSING OF RAYLEIGH-DISTRIBUTED FLUCTUATING TARGET

We begin with a single pulse processing ($M = 1$) of a Rayleigh-distributed fluctuating target. The analysis applies to both Swerling 1 and Swerling 2, since they differ in the degree of correlation between consecutive pulses only when $M > 1$. For a single pulse the (S + N)–N output can be expressed as

$$r^2 = \underbrace{\left[(A+n_{I1})^2+n_{Q1}^2\right]}_{a} + \underbrace{\left[-\left(n_{I2}^2+n_{Q2}^2\right)\right]}_{b}. \tag{19}$$

Here the amplitude A is a random variable (r. v.), taken from the Rayleigh pdf

$$p\,(A) = \frac{A}{A_0^2}\,e^{\frac{-A^2}{2A_0^2}}. \tag{20}$$

The average SNR $\bar{x}$ is obtained from the properties of the Rayleigh variable A

$$\bar{x} = \frac{\overline{A^2}}{2\sigma^2} = \frac{A_0^2}{\sigma^2}. \tag{21}$$

From (20) and (21) we obtain the pdf of x

$$p(x) = \frac{1}{\bar{x}} e^{\frac{-x}{\bar{x}}}. \tag{22}$$

Because the *a, b* parts of (19) are independent, the characteristic function can be written as

$$C_{ab|A}(\omega) = C_{a|A}(\omega) C_b(\omega). \tag{23}$$

For a single normalized detected pulse, the output y is

$$y = z = \frac{r^2}{2\sigma^2}. \tag{24}$$

We can now write

$$\begin{aligned} p(y) &= \int_{-\infty}^{\infty} p(y|x)\, p(x)\, dx \\ &= \int_{-\infty}^{\infty} \underbrace{\int_{0}^{\infty} C_{ab|A}(\omega) e^{j\omega y} d\omega}_{p(y|x)}\, p(x)\, dx \\ &= \int_{-\infty}^{\infty} \int_{0}^{\infty} C_{a|A}(\omega) C_b(\omega) e^{j\omega y} d\omega\, p(x)\, dx \\ &= \int_{0}^{\infty} e^{j\omega y} C_b(\omega) \underbrace{\int_{-\infty}^{\infty} C_{a|A}(\omega) p(x)\, dx}_{C_a}\, d\omega \\ &= \int_{0}^{\infty} e^{j\omega y} C_b(\omega) C_a(\omega)\, d\omega. \end{aligned} \tag{25}$$

Using (22) we get for the a part of (19)

$$C_a(\omega) = \frac{1}{1 + \omega(1 + \bar{x})}. \tag{26}$$

Using the definition

$$D = \frac{1}{1 + \bar{x}} \tag{27}$$

(26) becomes

$$C_a(\omega) = \frac{D}{D + \omega}. \tag{28}$$

$C_b(\omega)$ is obtained from setting $x = 0$ in (6). Thus the overall characteristic function becomes

$$C(\omega) = C_a(\omega) C_b(\omega) = \frac{D}{(D + \omega)(1 - \omega)}. \tag{29}$$

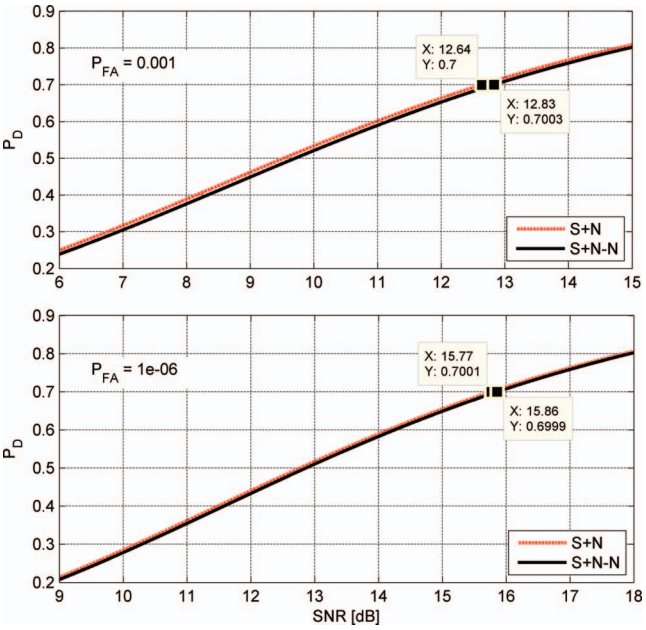

Fig. 3. Single-pulse detection performances for Rayleigh fluctuating target. (Top: $P_{\mathrm{FA}} = 10^{-3}$. Bottom: $P_{\mathrm{FA}} = 10^{-6}$).

As outlined in (25) we perform inverse Fourier transform of (29) getting the pdf of y

$$p(y) = \begin{cases} \frac{D}{1+D} e^{y} & y < 0 \\ \frac{D}{1+D} e^{-Dy} & y \geq 0 \end{cases}. \tag{30}$$

Setting $D = 1$ we get the pdf of y in the noise-only case

$$p_{\mathrm{noise}}(y) = \begin{cases} \frac{1}{2} e^{y} & y < 0 \\ \frac{1}{2} e^{-y} & \geq 0 \end{cases} = \frac{1}{2} e^{-|y|}. \tag{31}$$

The probability of false alarm for a positive threshold $y_T > 0$ becomes

$$P_{\mathrm{FA}} = \int_{y_T}^{\infty} \frac{1}{2} e^{-y} dy = \frac{1}{2} e^{-y_T}. \tag{32}$$

Finally, for a single Rayleigh-distributed pulse, (S + N)–N processing yields the relationship

$$P_D = \frac{1}{1 + D} (2P_{\mathrm{FA}})^D, \quad D = \frac{1}{1 + \overline{SNR}}. \tag{33}$$

For comparison note that in conventional noncoherent detection of a single Rayleigh-distributed pulse, the corresponding relationship is

$$P_D = (P_{\mathrm{FA}})^D. \tag{34}$$

In Fig. 3 the results of (33) and (34) are compared for two values of P_{FA}. The drawings show that in the case of a single pulse the SNR loss of (S + N)–N processing is less than 0.2 dB. This resembles Marcum's observation regarding nonfluctuating targets

. . . no significant difference in the probabilities of detection for M between 1 and 10 (pulses).

VI. $M > 1$, SWERLING 2

When dealing with integration of several pulses, the dependence between them matters, and we need to define the Swerling model. We begin with a Swerling 2 target, in which the reflected pulses are independent. The characteristic function of the sum of M independent r.v., when the individual pdf has the characteristic function in (29) is

$$C(\omega) = \frac{D^M}{[(D+\omega)(1-\omega)]^M}. \tag{35}$$

We show in Appendix A that the resulting pdf of the output y is given by

$$p(y) = \left(\frac{D}{1+D}\right)^M \frac{e^y (-y)^{M-1}}{(M-1)!} \begin{cases} \sum_{k=0}^{M-1} \left[\frac{(M+k-1)!}{k!(M-1-k)!}(-y(1+D))^{-k}\right], & y<0 \\ \sum_{k=0}^{M-1} \left[\frac{\Gamma(M+k,(1+D)y)}{k!(M-1-k)!}(-y(1+D))^{-k}\right], & y \geq 0 \end{cases} \tag{36}$$

where $\Gamma(a,x)$ is the upper incomplete gamma function (44).

VII. $M > 1$, SWERLING 1

The characteristic function of Swerling 0, according to (7), is

$$C(\omega) = \frac{e^{-Mx}}{(\omega+1)^M} \cdot e^{\frac{Mx}{\omega+1}}. \tag{37}$$

Following the Swerling approach [2] we average (37) over the SNR variable x, getting

$$C(\omega) = \frac{1}{(1+\omega)^{M-1}[1+\omega(1+M\bar{x})]}. \tag{38}$$

Using the procedure shown in (25) we get the final characteristic function

$$C(\omega) = \frac{1}{(1+\omega)^{M-1}[1+\omega(1+M\bar{x})]} \; \frac{1}{(1-\omega)^M}. \tag{39}$$

In Appendix B we perform the inverse transform and get the pdf of the integration output in the Swerling 1 case

$$p(y) = \begin{cases} \dfrac{\alpha e^y (-y)^{M-1}}{(M-1)!2^M} \displaystyle\sum_{k=0}^{M-1} \frac{(-y)^{-k}}{k!(M-1-k)!} \frac{\Gamma(k+M)}{2^k} {}_2F_1\left(1, k+M, M, \frac{1-\alpha}{2}\right), & y<0 \\ \dfrac{\alpha e^y}{(1-\alpha)^{M-1}} \displaystyle\sum_{k=0}^{M-1} \frac{(-y)^{M-1-k}}{k!(M-1-k)!} \left((1+\alpha)^{-k-1}\Gamma(k+1,(1+\alpha)y) - \sum_{m=0}^{M-2} \frac{(1-\alpha)^m}{m!} 2^{-k-m-1}\Gamma(k+m+1,2y)\right), & y \geq 0 \end{cases} \tag{40}$$

where ${}_2F_1()$ is Gauss hypergeometric function and

$$\alpha = \frac{1}{(1+M\bar{x})}. \tag{41}$$

VIII. NUMERICAL CALCULATIONS AND CONFIRMATION BY MONTE-CARLO RUNS

A. Swerling 2

The pdf given in (36) contains several factorials. MATLAB limits factorial calculations for arguments up to 170, and the accuracy drops before that value. To circumvent that limit we use the property

$$\Gamma(n) = (n-1)!. \tag{42}$$

We also use MATLAB's function gammaln which calculates the logarithm of the Gamma function. Denoting that logarithm as $\Gamma_{\ln}$, we use the relationship

$$\frac{(M+k-1)!}{(M-1)!k!(M-1-k)!} = \frac{\Gamma(M+k)}{\Gamma(M)\Gamma(k-1)\Gamma(M-k)}$$
$$= \exp[\Gamma_{\ln}(M+k) - \Gamma_{\ln}(M) - \Gamma_{\ln}(k-1) - \Gamma_{\ln}(M-k)]. \tag{43}$$

Note also the difference between the conventional definitions of the lower and upper incomplete gamma functions

$$\gamma(a,x) = \int_0^x e^{-t}t^{a-1}dt, \quad \Gamma(a,x) = \int_x^\infty e^{-t}t^{a-1}dt \tag{44}$$

and MATLAB's corresponding definitions of gammainc (x,a) and gammainc (x,a,tail)

$$P(a,x) = \frac{1}{\Gamma(a)}\int_0^x e^{-t}t^{a-1}dt, \; Q(a,x) = \frac{1}{\Gamma(a)}\int_x^\infty e^{-t}t^{a-1}dt. \tag{45}$$

After taking care of these issues we get good agreement between the closed-form expression (36) and Monte-Carlo simulations, as demonstrated in the example shown in Fig. 4.

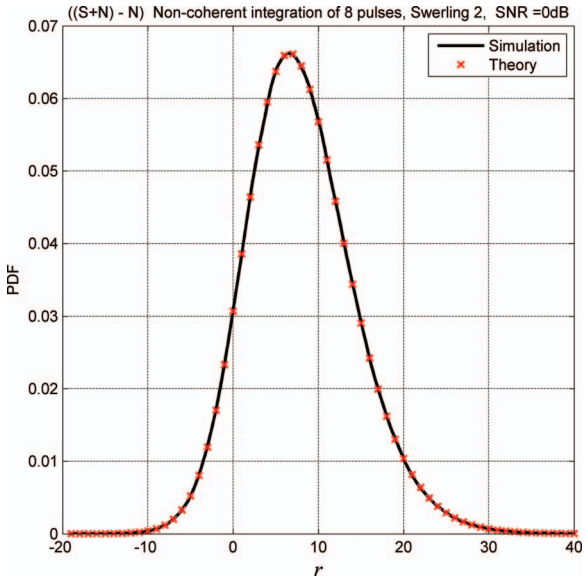

Fig. 4. PDF of (S + N)–N integration. SW2 case. Theory and simulations.

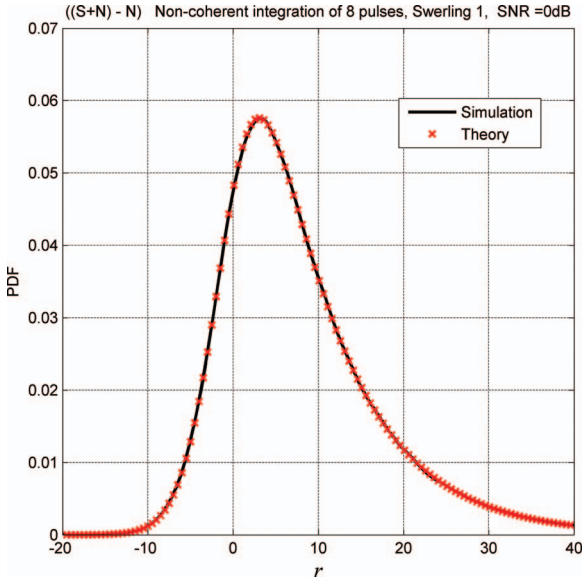

Fig. 5. PDF of (S + N)–N integration. SW1 case. Theory and simulations.

B. Swerling 1

Here we compare the closed-form expression in (40) with Monte-Carlo simulation. An example is given in Fig. 5. As in conventional noncoherent integration, note the longer tail of the Swerling 1 pdf. Having demonstrated the validity of the closed-form expressions, we next compare conventional noncoherent integration with the alternative integration.

IX. COMPARING MARCUM'S (S + N)–N AND CONVENTIONAL S + N NONCOHERENT INTEGRATIONS

We are interested in two aspects of the comparison: 1) the structure of the pdfs, especially of the noise-only

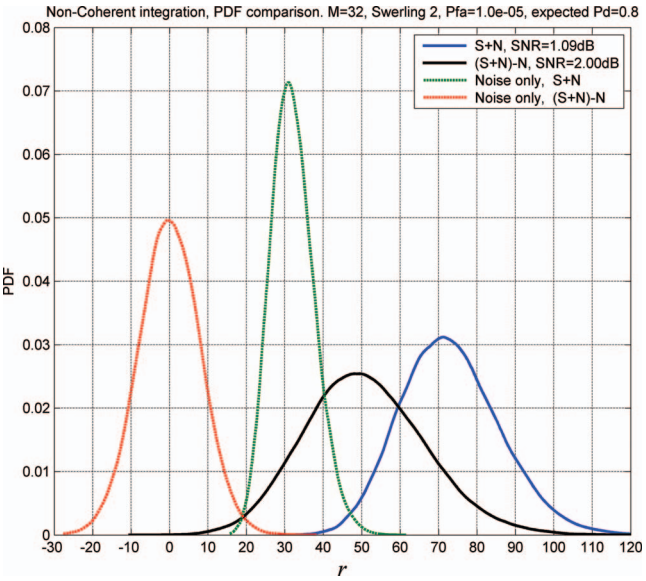

Fig. 6. PDFs of (S + N)–N and S + N integrations, SW2.

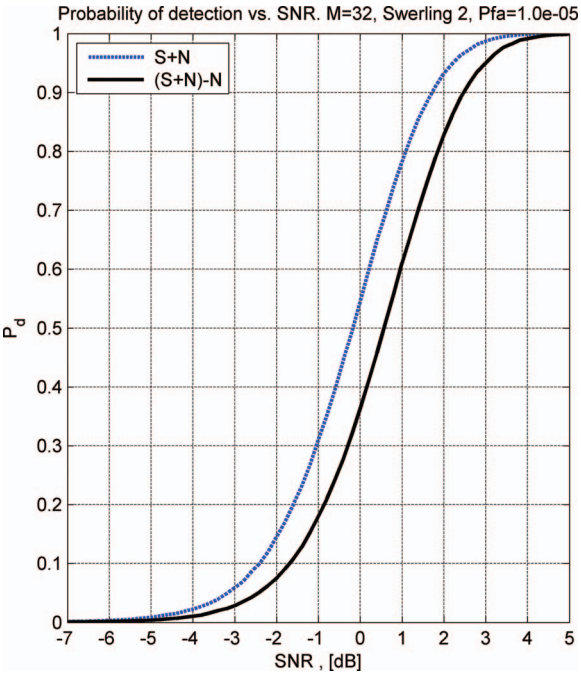

Fig. 7. P_D vs. SNR for (S + N)–N and S + N integrations, SW2.

case, and 2) the additional SNR loss of the (S + N)–N integration. For the Swerling 2 case the pdfs are shown in Fig. 6 and the P_D vs. SNR in Fig. 7. Both drawings apply to 32 pulses and $P_{FA} = 10^{-5}$. For the SW2 case Fig. 6 demonstrates how the noise-only pdf of N–N is centered around zero, and that the signal + noise pdf of (S + N)–N integration has also shifted toward zero. Fig. 7 shows an SNR loss of approximately 1dB for a wide range of P_D values. Fig. 8 displays the pdf plots for the Swerling 1 case, with its long-tailed signal + noise pdf. Here too the signal + noise pdf of the (S + N)–N integration shifts toward zero. The noise-only pdfs in Figs. 6 and 8 are, of

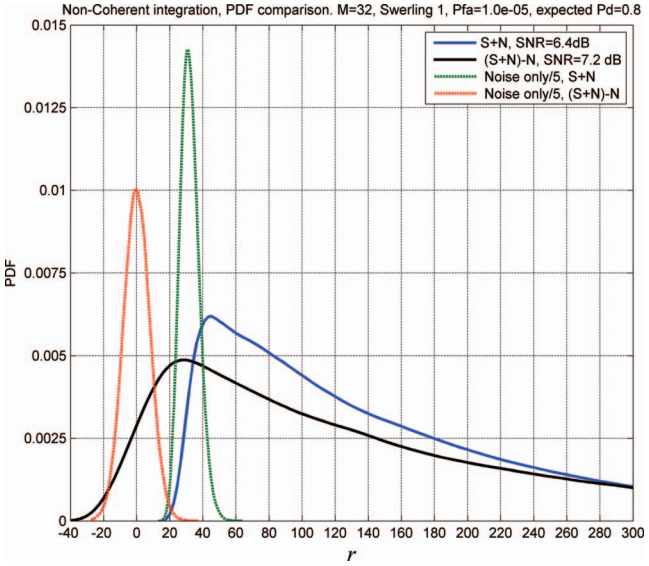

Fig. 8. PDFs of (S + N)–N and S + N integrations, SW1.

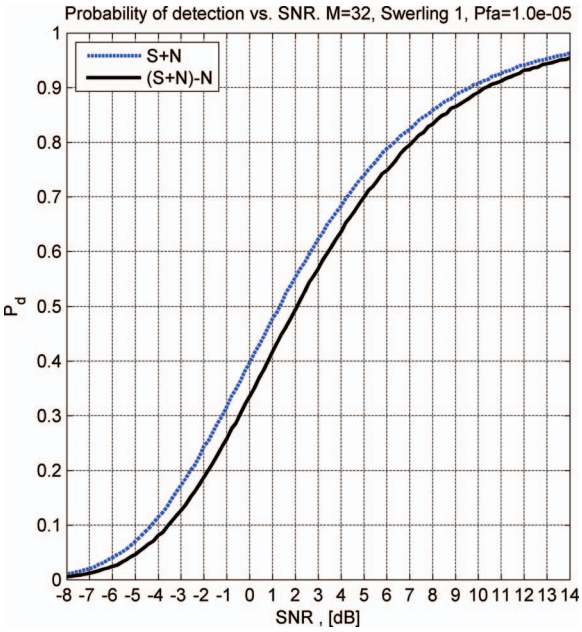

Fig. 9. P_D vs. SNR for (S + N)–N and S + N integrations, SW1.

course, identical. Fig. 9 shows that for SW1 the SNR loss is about 1 dB too. Fig. 10 extends the comparison to the nonfluctuating case (SW0). Fig. 10 also shows an SNR loss of about 1dB, as reported by Marcum.

X. SUMMARY AND DISCUSSION

Marcum's alternative noncoherent integration scheme of (S + N)–N, originally left out of Swerling's fluctuating target analysis, was now analyzed for Swerling 1 and 2 targets. Closed-form pdf expressions were derived and confirmed by simulations. The noise-only pdf of (S + N)–N integration is shown to be centered around zero. This is an important advantage for detection

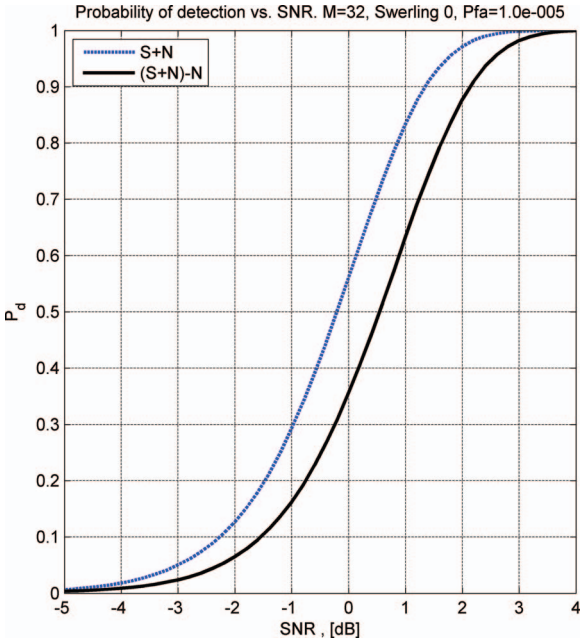

Fig. 10. P_D vs. SNR for (S + N)–N and S + N integrations, SW0.

threshold setting. We also showed that for both SW1 and SW2 targets the SNR loss of this alternative scheme is about 1 dB. The same loss was found by Marcum for nonfluctuating targets (SW0). Because SW3 (or SW4) describe a fluctuation model between SW0 and SW1 (or SW2), it is reasonable to expect a similar SNR loss of 1dB, in the SW3 and SW4 cases as well. Weighting the advantage of zero-centered output when detecting noise only, against the small SNR loss, Marcum's (S + N)–N integration warrants favorable reconsideration.

APPENDIX A

This Appendix shows the development of the pdf in (36) from its characteristic function in (35). We rewrite (35) as a product

$$C(\omega) = \frac{D^M}{(D+\omega)^M} \cdot \frac{1}{(1-\omega)^M} = C_1(\omega)\, C_2(\omega). \quad (46)$$

Each term in the product has a known inverse Fourier transform

$$p_1(y) = \begin{cases} \frac{D^M y^{M-1}}{(M-1)!} e^{-Dy}, & y \geq 0 \\ 0, & y < 0 \end{cases} \quad (47)$$

$$p_2(y) = \begin{cases} \frac{(-y)^{M-1}}{(M-1)!} e^{y}, & y < 0 \\ 0, & y \geq 0 \end{cases}. \quad (48)$$

The inverse transform of the product in (46) is obtained by convolving (47) with (48). We chose Y as the variable of

the resulting pdf.

$$p(Y)=\int_{Y}^{\infty}\frac{D^{M}y^{M-1}}{(M-1)!}e^{-Dy}U(y)\frac{(y-Y)^{M-1}}{(M-1)!}e^{Y-y}dy$$
$$=\frac{D^{M}e^{Y}}{[(M-1)!]^{2}}\int_{Y}^{\infty}y^{M-1}e^{-y(1+D)}\times(y-Y)^{M-1}U(y)\,dy. \tag{49}$$

For $Y<0$ the lower boundary of the integral is 0:

$$p(Y)=\frac{D^{M}e^{Y}}{[(M-1)!]^{2}}\times\int_{0}^{\infty}y^{M-1}e^{-y(1+D)}(y-Y)^{M-1}\,dy,\ \ Y<0. \tag{50}$$

We use Newton's binomial series to develop the expression $(y-Y)^{M-1}$

$$(y-Y)^{M-1}=\sum_{k=0}^{M-1}\frac{(M-1)!}{k!\,(M-1-k)!}y^{k}(-Y)^{M-1-k} \tag{51}$$

insert it in (50) and switch the order between integration and sum

$$p(Y)=\frac{D^{M}e^{Y}}{(M-1)!}\sum_{k=0}^{M-1}\frac{(-Y)^{M-1-k}}{k!\,(M-1-k)!}\times\int_{0}^{\infty}y^{M+k-1}e^{-y(1+D)}dy,\quad Y<0. \tag{52}$$

Solving the integral with the help of [8, eq. 3.351.3] we get

$$p(Y)=\frac{D^{M}e^{Y}}{(M-1)!}\sum_{k=0}^{M-1}\left[\begin{array}{l}\dfrac{(M+k-1)!}{k!\,(M-1-k)!}\\ \times(-Y)^{M-1-k}(1+D)^{-M-k}\end{array}\right] \tag{53}$$

which can be further simplified to yield the following two expressions

$$p(Y)=\left(\frac{D}{1+D}\right)^{M}\frac{e^{Y}(-Y)^{M-1}}{(M-1)!}\times\sum_{k=0}^{M-1}\left[\frac{(M+k-1)!}{k!\,(M-1-k)!}(-Y(1+D))^{-k}\right],\quad Y<0 \tag{54}$$

$$p(Y)=\frac{D^{M}e^{Y}}{(M-1)!}\sum_{k=0}^{M-1}\frac{(-Y)^{M-1-k}}{k!\,(M-1-k)!}\times\int_{Y}^{\infty}y^{M+k-1}e^{-y(1+D)}dy,\quad Y\geq 0. \tag{55}$$

To solve the integral in (55) we use [8, eq. 3.351.2], which says

$$\int_{Y}^{\infty}y^{n}e^{-\mu y}dy=\mu^{-n-1}\Gamma(n+1,\mu Y) \tag{56}$$

and get

$$p(Y)=\left(\frac{D}{1+D}\right)^{M}\frac{e^{Y}(-Y)^{M-1}}{(M-1)!}\times\sum_{k=0}^{M-1}\left[\frac{\Gamma(M+k,(1+D)Y)}{k!\,(M-1-k)!}(-Y(1+D))^{-k}\right],\quad Y\geq 0. \tag{57}$$

Exchanging Y with y in (54) and (57) produces the pdf in (36) for the Swerling 2 case.

APPENDIX B

This Appendix shows the development of the pdf in (40) for the Swerling 1 case. Recall that for the Swerling 0 case the characteristic function was given in (7) and is repeated below

$$C(\omega)=\frac{e^{-Mx}}{(\omega+1)^{M}}\cdot e^{\frac{Mx}{\omega+1}}. \tag{58}$$

Following the Swerling approach we average over the SNR x and get

$$C(\omega)=\frac{1}{(1+\omega)^{M-1}\cdot[1+\omega(1+M\bar{x})]}. \tag{59}$$

Using the conclusion described in (25) for our present problem we get the following characteristic function:

$$C(\omega)=\frac{1}{(1+\omega)^{M-1}\cdot[1+\omega(1+M\bar{x})]}\cdot\frac{1}{(1-\omega)^{M}} \tag{60}$$

which we split into two parts:

$$C_{1}(\omega)=\frac{1}{(1+\omega)^{M-1}\cdot[1+\omega(1+M\bar{x})]}$$
$$C_{2}(\omega)=\frac{1}{(1-\omega)^{M}}\ . \tag{61}$$

The inverse transform of $C_2(\omega)$ was obtained already in (48) as

$$p_{2}(y)=\begin{cases}\frac{(-y)^{M-1}}{(M-1)!}e^{y}, & y<0\\ 0, & y\geq 0\end{cases}. \tag{62}$$

Toward performing the inverse transform of $C_1(\omega)$ we define

$$\alpha=\frac{1}{(1+M\bar{x})} \tag{63}$$

and rewrite $C_1(\omega)$ as

$$C_{1}(\omega)=\frac{\alpha}{(1+\omega)^{M-1}\cdot[\alpha+\omega]}. \tag{64}$$

Using [9, eq. 581.7] we get

$$p_1(y) = \begin{cases} \frac{\alpha}{\Gamma(M-1)(1-\alpha)^{M-1}} e^{-\alpha y} \cdot \gamma[M-1,(1-\alpha)y], & y \geq 0 \\ 0, & y < 0 \end{cases}. \tag{65}$$

Using the property that a product in the Fourier domain (ω) is equivalent to convolution in the Y domain, we get the expression

$$p(Y) = \int_Y^\infty \frac{\alpha}{\Gamma(M-1)(1-\alpha)^{M-1}} e^{-\alpha y} \cdot \gamma[M-1,(1-\alpha)y] U(y) \frac{(y-Y)^{M-1}}{(M-1)!} e^{Y-y} dy \tag{66}$$

which can be simplified to

$$p(Y) = \frac{\alpha e^Y}{(M-1)!\ \Gamma(M-1)\ (1-\alpha)^{M-1}} \times \int_Y^\infty \gamma[M-1,(1-\alpha)y](y-Y)^{M-1} e^{-y(1+\alpha)} U(y) dy. \tag{67}$$

We again apply Newton's binomial series (51) to replace $(y-Y)^{M-1}$ in (67), and also switch the order between integration and sum to get

$$p(Y) = \frac{\alpha e^Y}{\Gamma(M-1)\cdot(1-\alpha)^{M-1}} \sum_{k=0}^{M-1} \frac{(-Y)^{M-1-k}}{k!(M-1-k)!} \times \int_Y^\infty \gamma[M-1,(1-\alpha)y] e^{-y(1+\alpha)} y^k U(y) dy. \tag{68}$$

For $Y < 0$ the lower boundary of the integral is 0. Next we use [8, eq. 6.455.2]

$$\int_0^\infty x^{\mu-1} e^{-\beta x} \gamma(v, \alpha x) dx = \frac{\alpha^v \Gamma(\mu+v)}{v(\alpha+\beta)^{\mu+v}} \times {}_2F_1\left(1, \mu+v, v+1, \frac{\alpha}{\alpha+\beta}\right) \tag{69}$$

and get

$$p(Y) = \frac{\alpha e^Y}{\Gamma(M-1)\cdot(1-\alpha)^{M-1}} \times \sum_{k=0}^{M-1} \frac{(-Y)^{M-1-k}}{k!(M-1-k)!} \frac{(1-\alpha)^{M-1}\Gamma(k+M)}{(M-1)2^{k+M}} \times {}_2F_1\left(1, k+M, M, \frac{1-\alpha}{2}\right) \tag{70}$$

which can be simplified to

$$p(Y) = \frac{\alpha e^Y (-Y)^{M-1}}{(M-1)!2^M} \sum_{k=0}^{M-1} \frac{(-Y)^{-k}}{k!(M-1-k)!} \frac{\Gamma(k+M)}{2^k} \times {}_2F_1\left(1, k+M, M, \frac{1-\alpha}{2}\right), \quad Y < 0. \tag{71}$$

For $Y \geq 0$ we have to solve the integral in

$$p(Y) = \frac{\alpha e^Y}{\Gamma(M-1)\cdot(1-\alpha)^{M-1}} \sum_{k=0}^{M-1} \frac{(-Y)^{M-1-k}}{k!(M-1-k)!} \times \int_Y^\infty \gamma[M-1,(1-\alpha)y] e^{-y(1+\alpha)} y^k U(y) dy. \tag{72}$$

The lower incomplete Gamma function γ [] can be expressed as given in [8, eq. 8.352.2]:

$$\gamma[M-1,(1-\alpha)y] = (M-2)! \times \left(1 - e^{-(1-\alpha)y} \sum_{m=0}^{M-2} \frac{((1-\alpha)y)^m}{m!}\right). \tag{73}$$

Using (73) in the integral in (72) it becomes

$$\int_Y^\infty \gamma[M-1,(1-\alpha)y] e^{-y(1+\alpha)} y^k U(y) dy = (M-2)! \int_Y^\infty \left(1 - e^{-(1-\alpha)y} \sum_{m=0}^{M-2} \frac{((1-\alpha)y)^m}{m!}\right) e^{-y(1+\alpha)} y^k dy. \tag{74}$$

The expression on the RHS of (74) can be simplified, excluding the $(M-2)!$ for the moment, as

$$\int_Y^\infty e^{-y(1+\alpha)} y^k dy - \int_Y^\infty e^{-2y} \sum_{m=0}^{M-2} \frac{((1-\alpha)y)^m}{m!} y^k dy. \tag{75}$$

The first term in (75) can be solved using [8, eq. 3.351.2], shown also in (56) above:

$$\int_Y^\infty e^{-y(1+\alpha)} y^k dy = (1+\alpha)^{-k-1} \Gamma(k+1, (1+\alpha)Y). \tag{76}$$

The second term in (75) can be rewritten as

$$\int_Y^\infty e^{-2y} \sum_{m=0}^{M-2} \frac{((1-\alpha)y)^m}{m!} y^k dy = \sum_{m=0}^{M-2} \frac{(1-\alpha)^m}{m!} \int_Y^\infty e^{-2y} y^{k+m} dy. \tag{77}$$

We again got the same type of integral, hence the final expression of the RHS of (74) is

$$(M-2)!\left((1+\alpha)^{-k-1}\Gamma(k+1,(1+\alpha)Y) - \sum_{m=0}^{M-2} \frac{(1-\alpha)^m}{m!} 2^{-k-m-1}\Gamma(k+m+1, 2Y)\right). \tag{78}$$

Inserting it in (72) we get the pdf for positive values:

$$p(Y) = \frac{\alpha e^{Y}}{(1-\alpha)^{M-1}} \sum_{k=0}^{M-1} \frac{(-Y)^{M-1-k}}{k!\,(M-1-k)!} \times \left((1+\alpha)^{-k-1}\,\Gamma(k+1,(1+\alpha)\,Y) - \sum_{m=0}^{M-2} \frac{(1-\alpha)^{m}}{m!} 2^{-k-m-1}\Gamma(k+m+1,2Y) \right), \quad Y \geq 0. \tag{79}$$

Combining (71) with (79) and replacing Y with y yields the pdf expression for the Swerling 1 case, given in (40).

REFERENCES

[1] Marcum, J. I.
A statistical theory of target detection by pulsed radar. RAND Corp. Res. Mem. RM-754, 1 Dec. 1947.
Reprinted in the *IRE Transactions on Information Theory*, **6**, 2, (1960), 59–267.

[2] Swerling, P.
Probability of detection for fluctuating targets. RAND Corp. Res. Mem. RM-1217, 17 March. 1954.
Reprinted in the *IRE Transactions on Information Theory*, **6**, 2 (1960), 269–308.

[3] Levanon, N.
Noncoherent pulse compression.
IEEE Transactions on Aerospace and Electronic Systems, **42**, 2 (2006), 756–765.

[4] Peer, U., and Levanon, N.
Compression waveforms for non-coherent radar.
IEEE Radar Conference, 2007, Boston, MA, USA, April 17-20, 2007.

[5] Levanon, N., Ben-Yaacov, E., and Quartler, D.
New waveform for magnetron marine radar - experimental results.
IET Radar Sonar Navigation, **6**, 5 (2012), 314–321.

[6] Kravitz, D., Grodensky, D., Levanon, N., and Zadok, A.
High-resolution low-sidelobes laser ranging based on incoherent pulse-compression.
IEEE Photonics Technology Letters, **24**, 23, (December 1, 2012), 2119–2121.

[7] Chernyak, V.
On a closed form for the noncoherent gain factor.
IEEE Transactions on Aerospace and Electronic Systems, **48**, 2 (April 2012), 1770–1771.

[8] Gradshteyn, I. S., and Ryzhik, I. M.
Table of Integrals, Series, and Products, Seventh Edition.
Elsevier, 2007.

[9] Campbell, G. A. and Foster, R. M.
Fourier Integrals for Practical Applications. Bell Telephone System, Monograph B-**584**, September 1931.

Alexander Sadogursky (S'06- M'12) was born in Kishinev, Moldova, on February 1, 1984. He received the B.Sc. in electrical and computer engineering from Ben Gurion University, Israel, in 2006, and the M.Sc. degree in electrical engineering from Tel-Aviv University, Israel in 2012. His current position is at Marvell Semiconductor Israel Ltd.

Nadav Levanon (S'67-M'70-SM'83-F'98-LF'06) was born in Israel in 1940. He received his B.Sc. (1961) and M.Sc. (1965) in electrical engineering from the Technion, Haifa, Israel, and the Ph.D. (1969) in electrical and computer engineering from the University of Wisconsin – Madison.

He is professor emeritus at Tel Aviv University, Israel, where he has been a faculty member since 1970. He was Chairman of the EE-Systems Department during 1983-1985, incumbent of the chair on Radar, Navigation and Electronic Systems and head of the Weinstein Research Institute for Signal Processing. He spent sabbatical years at the University of Wisconsin, The Johns Hopkins University - Applied Physics Laboratory, and Qualcomm Inc, San Diego.

Dr. Levanon is a Life Fellow of the IEEE. His 1998 fellow citation is for "Contributions to radar signal analysis and detection". He is also a Fellow of the IET and member of the ION and AGU. He is the author of the book *Radar Principles* (Wiley, 1988) and co-author of *Radar Signals* (Wiley, 2004).